Thin Solid Films 690 (2019) 137532

Contents lists available at ScienceDirect

Thin Solid Films

journal homepage: www.elsevier.com/locate/tsf

Thin films of $(Ag_xCu_{1-x})_2ZnSn(S,Se)_4$ (x = 0.05–0.20) prepared by spray pyrolysis

L. Dermenji[a], M. Guc[a,*], G. Gurieva[b], Th. Dittrich[c], J. Rappich[c], N. Curmei[a], L. Bruc[a], D.A. Sherban[a], A.V. Simashkevich[a], S. Schorr[b,d], E. Arushanov[a]

[a] Institute of Applied Physics, str. Academiei 5, MD-2028, Chisinau, Republic of Moldova
[b] Helmholtz-Zentrum Berlin für Materialien und Energie GmbH, Abteilung Struktur und Dynamik von Energiematerialien, Hahn-Meitner-Platz 1, 14109 Berlin, Germany
[c] Helmholtz-Zentrum Berlin für Materialien und Energie GmbH, Institut für Si-Photovoltaik, Kekuléstr. 5, D-12489 Berlin, Germany
[d] Institute of Geological Sciences, Free University Berlin, Malteserstr. 74-100, 12249 Berlin, Germany

ARTICLE INFO

Keywords:
Kesterite
Solid solution
Spray pyrolysis
Energy dispersive X-ray spectroscopy
Grazing incidence X-ray diffraction
Raman scattering
Surface photovoltage
Electrical properties

ABSTRACT

The recent investigation of kesterite type quaternary compounds showed that one of the main detrimental problems, which limits the efficiency of the solar cells based on these materials, is related to the high defect concentrations, mainly Cu−Zn disorder. To overcome this problem partial replacement of Cu or Zn cations in the classical $Cu_2ZnSn(S,Se)_4$ compounds was proposed. One of the promising cations was found to be Ag, which partially replaces Cu and the solid solution of $(Ag_xCu_{1-x})_2ZnSn(S,Se)_4$ (ACZTSSe) is formed. In the present study, ACZTSSe thin films with different Ag concentrations were deposited by the spray pyrolysis method, with subsequent annealing in S + Se atmosphere. From the analysis of the chemical composition of the thin films a good correlation of measured silver concentration with initial concentration (dissolved in the main solution for deposition) for the samples with up to 15% Ag were found. These results were also confirmed by the structural studies and analysis of the Raman scattering spectra. On the other hand, thin film with higher Ag concentration (20%) has shown strong compositional inhomogeneity and presence of secondary phases was detected. Analysis of the modulated surface photo-voltage yielded the optical transition at ~ 1.5 eV, correlated with the band gap energy, and a transition at lower energy. From the temperature dependence of resistivity investigation no significant change in the resistivity for the samples with low silver concentration and strong increase for the samples with 20% of Ag were found.

1. Introduction

$Cu_2ZnSn(S,Se)_4$ (CZTSSe) quaternary compounds have been considered recently as promising materials for the development of cheap and effective thin-film solar cells. This is mainly due to abundant and non-toxic elements which constitute this compounds. Some of the scientific groups managed to produce high efficient solar cells based on quaternary compounds [1–5] and the maximum energy conversion factor in the laboratory exceeded 12% [5]. However, further improvements have stopped due to the low open circuit voltage (V_{oc}). The latter, according to many theoretical and experimental studies, is mostly related to the high concentration of intrinsic defects, leading to a low minority carrier lifetime, electrostatic potential fluctuations, tail states etc. [6–8]. The main defect is related with Zn_{Cu} anti-sites, which leads to the creation of the defect acceptor band inside the band gap [9–11]. Predominance of this defect is insured by the low formation energy, which could be explained by the small difference in the sizes of atoms and chemical properties of Cu and Zn [12,13]. In this context several compounds with partial replacement of Cu or Zn cations were proposed [14–16]. Ag was proposed as a promising candidate for substitution of Cu, since it belongs to the same chemical group as copper, but its radius is 16% larger, which should lead to an increase in the formation energy of Zn/Ag disorder [17–22]. However, pure $Ag_2ZnSn(S,Se)_4$ (AZTSSe) is a semiconductor with n-type conductivity, which assumes certain changes in the thin film solar cell architecture [23]. Therefore, it is necessary to consider the transition series of solid solutions from CZTSSe to AZTSSe in order to overcome the difficulties arising in CZTSSe and AZTSSe end members of this solid solution. Recently, the spray pyrolysis deposition was used as fast and easy scalable technique for obtaining not only CZTSSe compounds, but also the Ag containing solid solutions [24–26]. Data on structural, compositional, morphological and vibrational properties were presented [24–26], and

* Corresponding author.
E-mail address: mguc@irec.cat (M. Guc).

https://doi.org/10.1016/j.tsf.2019.137532
Received 22 August 2018; Received in revised form 29 June 2019; Accepted 28 August 2019
Available online 28 August 2019

a positive influence of the Ag incorporation to the solar cells performance was shown by many authors [18–22,24–26]. However, in most of the published articles structural analysis was limited by the short angular range, only few details were given on vibrational Raman spectra and no analysis of electrical properties were presented.

In the present study thin films of $(Ag_xCu_{1-x})_2ZnSn(S,Se)_4$ (ACZTSSe), with x = 0.05–0.20, solid solutions were obtained by the non-vacuum spray pyrolysis method. In this way, the positive influence of Ag on the intrinsic defects of kesterite type compounds was combined with one of the easiest and cheapest deposition methods. For the obtained thin films the chemical composition and structural properties have been studied using energy dispersive X-ray microscopy (EDX) and grazing incidence X-ray diffraction (GIXRD) respectively, as well as Raman scattering spectroscopy. Additionally, the modulated surface photovoltage (SPV) and the temperature dependence of conductivity were analyzed in the thin films with different Ag concentration.

2. Materials and methods

2.1. Thin film preparation

The method of the tree source precursors (S1, S2 and S3) was used for the ACZTS thin films preparation. S1 contains Cu-complexes, S3 contains Ag-complexes and S2 contains Zn- and Sn-complexes. The S1 and S2 precursors are very stable and homogeneous (single phase) for long time in a large range of temperatures. The S3 precursor is also stable and homogeneous, but due to the high photosensitivity of the complex it should be kept in the conditions of darkness.

The S1 precursor was prepared in a similar way to that used for the Cu_2ZnSnS_4 preparation [27]. To the 17 ml of H_2O 2.3 mg of Thiourea $(CS(NH_2)_2)$ were added. The Thiourea was dissolved at the temperature of 32–38°C under a constant stirring. Afterwards 0.83 g of CuCl was added and stirred up to 3 h. The concentrations were selected considering that in the S1 precursor should contain 8.38 mmol of Cu^{+1}. Cooling of this precursor to temperatures < 25°C is leading to crystals precipitation in the solution, which can be easily dissolved by heating with stirring. The reason for this crystallization effect is the concentration of Thiourea, which is close to the solubility limit under the ambient condition and the limit could be crossed with decreasing of temperature of the solution.

To obtain the S2 precursor, 1.9 g of $CS(NH_2)_2$ was dissolved in the 17 ml of H_2O. Afterwards 4.38 g of $SnCl_4 \times 5H_2O$ and 2.75 g of Zn $(CH_3COO)_2 \times 2H_2O$ were added consecutively. The total volume of the solution was increased up to 25 ml by adding the H_2O.

The S3 precursor was obtained by dissolving the 1.9 g of Thiourea and 0.4 g of AgCl in 15 ml of H_2O. To increase the dissolving speed the solution temperature was kept in the range 30–35°C with the constant stirring. AgCl – is photosensitive (decomposes at the light), therefore all of the procedures were carried out in darkness, in order to avoid precipitation of metallic silver.

The main solution (MS) is prepared directly before the deposition. The ratio between the S1, S2 and S3 is usually S1':S2 = 3:1 in order to obtain a stoichiometric mixture of precursors. Here the S1' precursor was obtained by adding a different amount of the S3 precursor to the S1 in order to achieve the required Ag/Cu ratio. The obtained undiluted MS has a concentration of 0.33 M and the MS diluted with water has a molar concentration of 0.06 M.

The deposition of the thin layers of $(Ag_xCu_{1-x})_2ZnSnS_4$ was performed using the method of spray pyrolysis in the atmosphere of carbon dioxide at temperatures of 270–280 °C. The oxygen-free atmosphere allows excluding the oxidation reactions of the kesterite components and molybdenum contact at the glass substrate during the pyrolysis. Two sister samples were obtained during each deposition procedure: the first on soda-lime glass (SLG) substrate and the second on molybdenum coated SLG substrate. The latter was used for the subsequent deposition of CdS to obtain the p-n junction. To increase the crystalline quality of the films annealing process in an S + Se atmosphere at 525 °C for 30 min was performed in accordance with the parameters described for the Ag free system [27]. Note that, similar post-deposition annealing conditions were applied in Refs. [24, 25], however the higher substrate temperatures (380 °C [24], 350 °C [25]) were used during the deposition process.

2.2. Characterization techniques

The composition of the deposited thin films was analyzed using the energy dispersive X-ray microscopy (EDX). The INCAPentaFETx-3 Oxford Instruments EDX detector attached to the scanning electron microscope VEGA TS 5130 was used for this purpose. The thin films thickness was measured by using the interferometer Surtronic 25 from Taylor Hobson and the obtained values were in the range 0.9–1.2 μm, without any correlation with Ag content. The structural characterization of the thin films was carried out by grazing incidence X-ray diffraction (GIXRD) using a PANalytical X'pertPro MPD diffractometer equipped with CuKα radiation (λ = 1.54056 Å). The samples have been measured at 4 incidence angles ω = 0.5°, 1°, 2°, 5° allowing us to conclude on the in-depth homogeneity of the films. Raman scattering spectra were obtained with a Dilor LabRam micro Raman spectrometer coupled with a CCD camera and excited by a HeNe laser (632.8 nm). The excitation with 325 nm laser line was used for better detection of possible secondary phases in analyzed thin films. The SPV spectra were excited with a quartz prism monochromator (SPM2). The modulation frequency was 10 Hz. The modulated SPV spectra were measured in the fixed capacitor arrangement [28] with a double phase lock-in amplifier (EG&G 7260). In-phase and phase-shifted by 90° signals correspond to the fast and slow response in relation to the modulation period, respectively. The temperature dependence of the resistivity, ρ(T), was measured between 10 and 300 K by the Van der Pauw method using In contacts. The sample was placed in a closed circle helium cryostat to control the temperature. The hot probe method showed that all the investigated thin films had p-type conductivity.

3. Thin films characterization

The samples composition was measured in at least five points and the mean results are collected in Table 1. The elements concentrations for all samples were found to be close to stoichiometry. In Fig. 1 the dependence of the initial Ag concentration (Ag concentration dissolved in the solution) and the measured Ag concentration in the thin films is presented. As it can be seen, up to 15% Ag the measured value is very close to the initial concentration. With increasing the Ag concentration up to 20% strong inhomogeneity of the Ag distribution in the thin film was found and this resulted in a lower average value in the measured points. This could be related to some problems during the dissolution of higher amounts of the S3 precursor in the S1. As it was mentioned in the previous section, annealing of the thin films was performed in the S + Se atmosphere. This led to a partial sample selenization with an average Se/(Se + S) ≈ 0.13.

The GIXRD patterns in Fig. 2a show distinguishable Bragg reflexes, allowing to assign the most intensive peaks to the tetragonal ACZT(S,Se) – marked with stars, while starting with 15% content of Ag

Table 1
Chemical composition of the ACZTSSe thin films.

Sample	Ag (at.%)	Cu (at.%)	Zn (at.%)	Sn (at.%)	S (at.%)	Se (at.%)	Ag/(Ag + Cu)	Se/(Se + S)
ACZTSSe-5	1	23	14	12	44	6	0.05	0.12
ACZTSSe-10	2	22	13	13	44	7	0.10	0.13
ACZTSSe-15	4	21	11	13	45	7	0.15	0.13
ACZTSSe-20	3	22	13	13	43	6	0.13	0.13

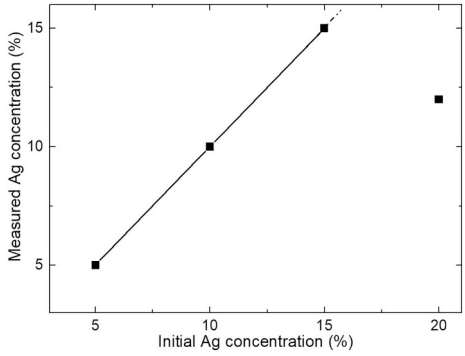

Fig. 1. Dependence of the measured by EDX Ag concentration from the initial concentration (the Ag concentration dissolved in the main solution).

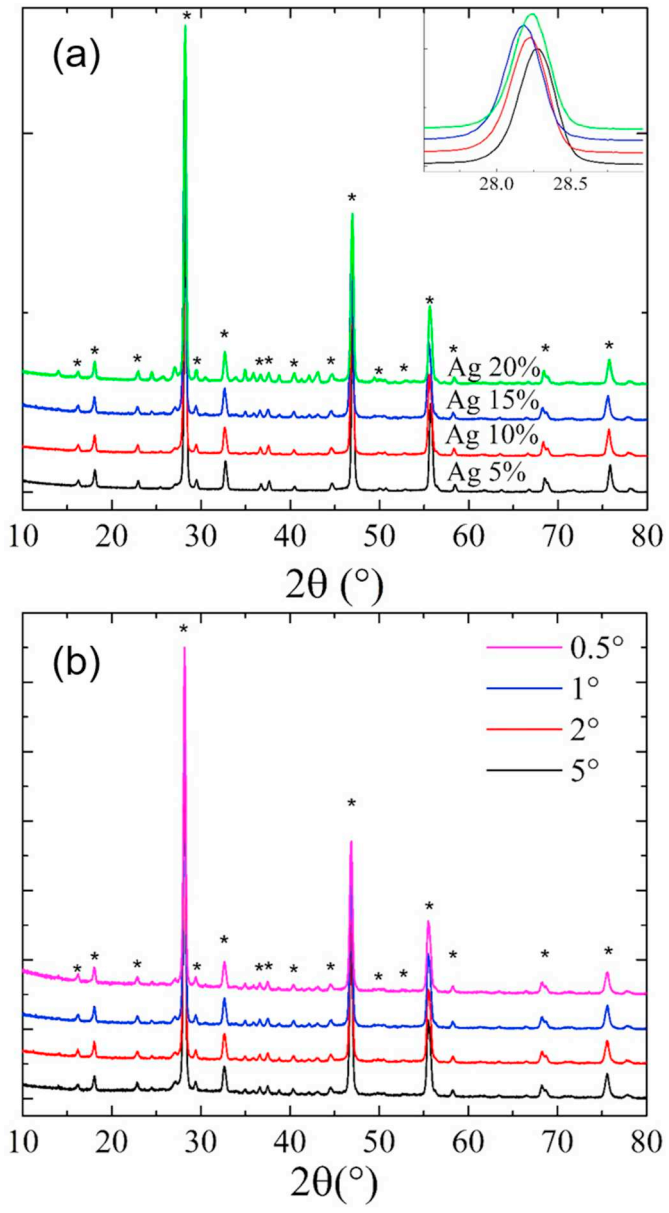

Fig. 2. (a) GIXRD patterns of the analyzed $(Ag_xCu_{1-x})_2ZnSn(S,Se)_4$ thin films; (b) measurements with 4 different incidence angles exemplarily shown for Ag 15% sample. In both plots the stars are indicating the peaks attributed to $(Ag_xCu_{1-x})_2ZnSn(S,Se)_4$ phase the non-indicated rest of the peaks belong to $Ag_8Sn(S,Se)_6$ secondary phase.

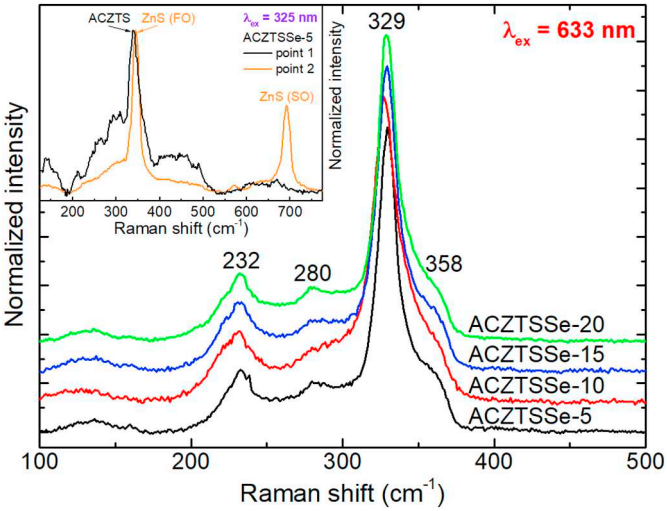

Fig. 3. Raman scattering spectra of the ACZTSSe thin films with different Ag concentration measured under 633 nm excitation. The inset shows the examples of the spectra obtained under UV excitation at different point of thin film with 5% Ag.

the presence of the ternary orthorhombic $Ag_8Sn(S,Se)_6$ secondary phase (all of the non-marked peaks) becomes visible. The very pronounced presence of this phase could be the reason for the observed discrepancy between initial and measured composition of the 20% Ag film. Using Rietveld refinement, lattice constants of the main phase were derived, and Se/(Se + S) ratios of ~ 0.10–0.13 for all of the samples was obtained, which is in a satisfactory agreement with the values obtained from EDX measurements. As an additional in-depth homogeneity test all of the films were measured at 4 different incidence angles, the measurements for the sample with 15% Ag is exemplarily shown in Fig. 2b, proving no change in the diffraction patterns in dependence of the incidence angle.

In the Raman backscattering spectra only peaks characteristic for the kesterite type compounds were detected [29,30]. The low widths of the most intense peaks in the spectra denote the high crystalline quality of the analyzed samples (Fig. 3). However, a shift of the main peak to the lower wavenumber and insignificant increase of its width, together with decreased intensity of peak at 280 cm^{-1} in case of thin film with 10% of Ag, yield a bit lower crystalline quality for this sample. The small red shift of the most intense peak and appearance of the peaks close to 232 cm^{-1} is related to the formation of a sulfo-selenide solid solution [31]. Using the results from the Ref. [31], the relative ratio of Se in the analyzed samples was found and is close to that obtained from the compositional and structural analysis. On the other hand, there was no influence of the Ag cations on the Raman spectra observed. This is in line with the previously published results on Raman scattering analysis of kesterite solid solution samples with Ag [21,22,25]. The effect could be explained by the nature of the most intense Raman peaks in the kesterite type compounds, which is related to the anions vibrations [32] and the peaks position does not change significantly with cations replacement [33]. The Raman peaks of the secondary phase $Ag_8Sn(S,Se)_6$, found in some samples according to the GIXRD analysis, were not detected. This could be explained by their low intensity and strong overlap with the peaks of main kesterite phase [34]. Under the UV excitation the ZnS secondary phase was found in all thin films. However, the peaks of ZnS were found only in some points of the samples (see the inset of Fig. 3), thus no significant influence of this secondary phase is expected to the results presented below. The existence of other secondary phases (Cu_xS, SnS, Cu_2SnS_3) could be excluded or their concentrations are negligibly small.

The deposited ACZTSSe thin films with a CdS charge-selective contact were investigated for the first time by modulated surface

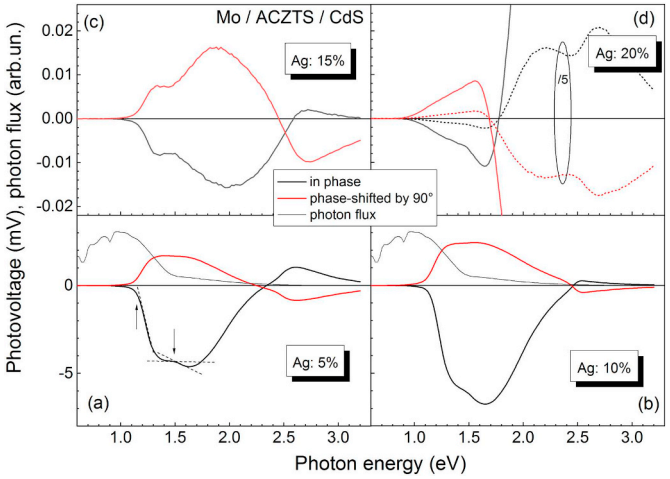

Fig. 4. In-phase (black lines) and phase-shifted by 90° (red lines) SPV spectra of ACZTSSe thin films with 5, 10, 15 and 20% Ag ((a) – (d), respectively). The short-dashed black and red lines give the spectra divided by 5 (d). The thin solid lines show the spectrum of the photon flux. The dashed lines and arrows give examples for the determination of onset energies. (For interpretation of the references to colour in this figure legend, the reader is referred to the web version of this article.)

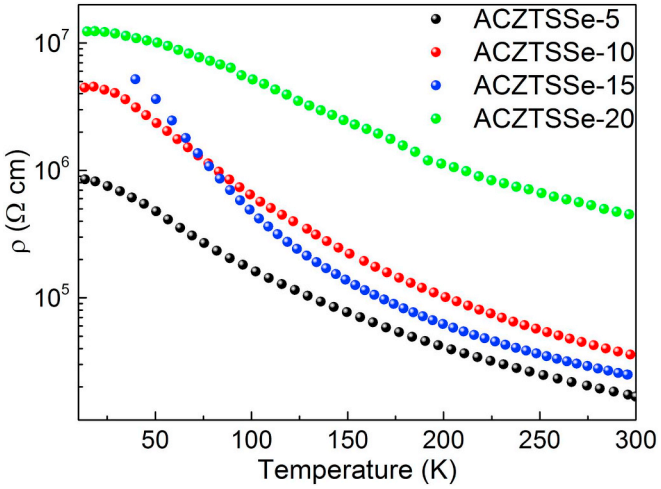

Fig. 5. Temperature dependence of the resistivity in ACZTSSe thin films.

photovoltage (SPV) spectroscopy in order to get information about the band gap. Fig. 4 shows the in-phase (x) and phase-shifted by 90° (y) SPV spectra for annealed ACZTSSe thin films containing 5, 10, 15 and 20% of Ag. The spectra set on at photon energies between about 0.9 and 1.2 eV. The in-phase signals (x) were negative and the phase-shifted by 90° signals (y) were positive in the range near the band gap what is typical for a p-type semiconductor in depletion with one dominating mechanism of charge separation and relaxation. Signatures related to the onset of photo-generation in CdS around 2.4 eV can be clearly distinguished in both SPV spectra. A further transition was observed at 1.5 eV for all sample. The sign of the x- and y-signals changed in the region of the band gap of CdS. In contrast, for the sample with 20% Ag, the sign of the x- and y-signals changed around 1.775 and 1.690 eV, respectively. This gives evidence for the formation of an additional n-type interlayer between the CdS and the ACZTS film.

An onset energy (E_{on}) can be defined as the approximation of the tangent in the inflection point to the zero signal. The onset energies are close but below the band gap. The values of $E_{on,x}$ and $E_{on,y}$ were 1.148 and 1.123 eV, 1.144 and 1.090 eV, 1.147 and 1.13 eV and 0.98 and 0.93 eV, respectively, for 5, 10, 15 and 20% Ag, respectively. The transition at 1.5 eV for all samples is comparable to the band gap of the analyzed thin films, taking into account both Ag and Se influence [19–23]. On the other hand, the nature of the low energy values found close to 1.1–1.2 eV is discussable. The secondary phase $Ag_8Sn(S,Se)_6$ could be responsible for this low band gap value [34]. However, from the GIXRD analysis this phase was found to be residual in the thin film with 10% Ag concentration, and disappeared for the thin film with 5% Ag concentration. Also, both Raman scattering spectroscopy and structural analysis showed the absence of any other secondary phases in the analyzed thin films, which have the band gaps in the range 1.1–1.2 eV. Another explanation of the low energy values could be connected to creation of deep defect level, which was found to be formed in some kesterite type compounds [35,36]. Furthermore, the origin and the composition of the interlayer between CdS and ACZTS for the sample with 20% is not clear yet. More detailed study of this question should be performed to be sure about the nature of low energy optical transitions in deposited ACZTSSe thin films.

The temperature dependence of resistivity showed an activated character over the whole measured range (Fig. 5). The dependencies obtained for the thin films with Ag concentrations up to 15% were found to be quite similar. At the same time, for the sample with the highest Ag concentration a strong increase of the resistivity value at any temperature comparing to other samples was found (see Fig. 5). It should be mentioned, that some saturation of the resistivity at low temperatures in case of some samples is rather related to the used installation limits of measurement than to the real change of resistivity dependence in the samples.

The obtained temperature dependencies of resistivity were analyzed in the way proposed previously in Refs. [37, 38] for the pure CZTS thin films. As a result, only the region with Mott type of variable-range hopping (Mott VRH) was found in the analyzed samples (see Fig. 6). From the analysis of Mott VRH the width of the acceptor band W [9] was found to decrease with increasing Ag concentration up to 15% (from 116 to 86 meV). This could be related to the different proximity of the thin films to the metal-insulator transition (MIT). The later was estimated using the universal Mott criterion and equations for the localization radius in proximity to the MIT (for more details see Refs. [9–11]). The value of relative acceptor concentration N/N_c (N_c is the critical acceptor concentration for the MIT) was found to change from 0.37 for the thin film containing 5% Ag to 0.27 for the thin film containing 15% Ag, indicating the above assumed difference in the proximity of the samples to the MIT. Generally, the thin films were found to be quite far from the MIT, which is similar to previously published results [38]. Here, a shift out of the MIT after the thermal treatment was

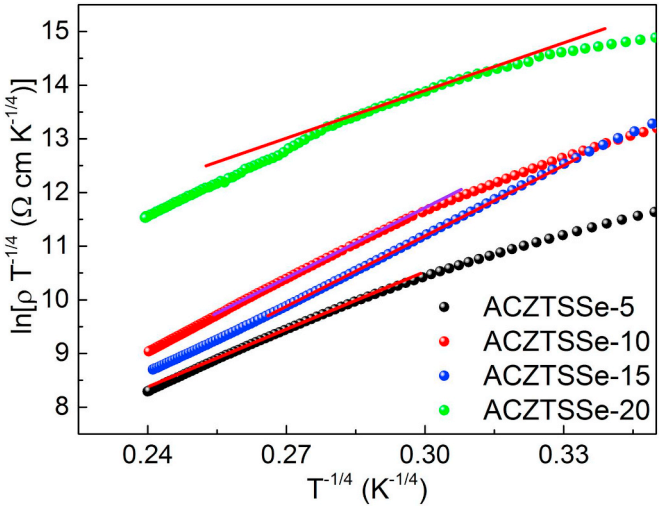

Fig. 6. Plots of $\ln(\rho/T^{1/4})$ vs. $T^{-1/4}$ addressed to the investigated thin films. The straight lines are linear fits.

observed, which was related to an increase of the structural disorder, while the acceptor concentration was decreased [38]. Finally, for the thin film with the highest Ag concentration $W = 63$ meV and $N/N_c = 0.41$. However, this result could be strongly influenced by the compositional inhomogeneity and the secondary phases, found from the compositional and structural analysis above. It is worth mentioning that no previously published results on analysis of temperature dependence of resistivity in ACZTSSe thin films were found.

4. Conclusions

In the presented study the ACZTSSe thin films with different Ag concentrations were deposited by the spray pyrolysis method, with subsequent annealing in S + Se atmosphere. From the analysis of the chemical composition of the thin films a good correlation of the measured Ag concentration with the initial concentration for thin films with up to 15% Ag was found. Further increase of the Ag concentration resulted in appearance of the strong compositional inhomogeneity, which could be related to a poor dissolving of the Ag containing precursor in the main solution used for the deposition. The formation of ACZTSSe solid solutions was proved by the structural studies and Raman backscattering analysis for the thin films with an Ag concentration up to 15%, while the evident existence of secondary phases was observed for the samples with higher Ag concentration. From the investigation of the temperature dependence of resistivity no significant change in the resistivity value for the thin films with low Ag concentration was found, while a strong increase of resistivity for the thin film with 20% Ag was observed. The latter could be related to the influence of the Ag_8SnSe_6 secondary phase and the compositional inhomogeneity found in this thin film.

Declaration of Competing Interest

None.

Acknowledgments

The research leading to the presented results has been partially supported by the INFINITE-CELL project. This project has received funding from the European Union's Horizon 2020 research and innovation program under the Marie Skłodowska-Curie grant agreement No 777968. Authors from IAP also appreciate the financial supports from STCU 6224 and from the Institutional Project CSSDT 15.817.02.04A.

References

[1] M. Buffiere, G. Brammertz, M. Batuk, C. Verbist, D. Mangin, C. Koble, J. Hadermann, M. Meuris, J. Poortmans, Microstructural analysis of 9.7% efficient $Cu_2ZnSnSe_4$ thin film solar cells, Appl. Phys. Lett. 105 (2014) 183903, , https://doi.org/10.1063/1.4901401.

[2] C.J. Hages, S. Levcenco, C.K. Miskin, J.H. Alsmeier, D. Abou-Ras, R.G. Wilks, M. Bär, T. Unold, R. Agrawal, Improved performance of Ge-alloyed CZTGeSSe thinfilm solar cells through control of elemental losses, Prog. Photovolt. Res. Appl. 23 (2015) 376–384, https://doi.org/10.1002/pip.2442.

[3] S. Giraldo, M. Neuschitzer, T. Thersleff, S. López-Marino, Y. Sánchez, H. Xie, M. Colina, M. Placidi, P. Pistor, V. Izquierdo-Roca, K. Leifer, A. Pérez-Rodríguez, E. Saucedo, Large efficiency improvement in $Cu_2ZnSnSe_4$ solar cells by introducing a superficial Ge nanolayer, Adv. Energy Mater. 5 (2015) 1501070, , https://doi.org/10.1002/aenm.201501070.

[4] K. Sun, C. Yan, F. Liu, J. Huang, F. Zhou, J.A. Stride, M. Green, X. Hao, Over 9% efficient kesterite Cu_2ZnSnS_4 solar cell fabricated by using $Zn_{1-x}Cd_xS$ buffer layer, Adv. Energy Mater. 6 (2016) 1600046, , https://doi.org/10.1002/aenm.201600046.

[5] J. Kim, H. Hiroi, T.K. Todorov, O. Gunawan, M. Kuwahara, T. Gokmen, D. Nair, M. Hopstaken, B. Shin, Y.S. Lee, W. Wang, H. Sugimoto, D.B. Mitzi, High efficiency $Cu_2ZnSn(S,Se)_4$ solar cells by applying a double In_2S_3/CdS emitter, Adv. Mater. 26 (2014) 7427–7431, https://doi.org/10.1002/adma.201402373.

[6] O. Gunawan, T.K. Todorov, D.B. Mitzi, Loss mechanisms in hydrazine-processed $Cu_2ZnSn(se,S)_4$ solar cells, Appl. Phys. Lett. 97 (2010) 233506, , https://doi.org/10.1063/1.3522884.

[7] I.L. Repins, H. Moutinho, S.G. Choi, A. Kanevce, D. Kuciauskas, P. Dippo, C.L. Beall, J. Carapella, C. DeHart, B. Huang, S.H. Wei, Indications of short minority-carrier lifetime in kesterite solar cells, J. Appl. Phys. 114 (2013) 084507, , https://doi.org/10.1063/1.4819849.

[8] T. Gokmen, O. Gunawan, T.K. Todorov, D.B. Mitzi, Band tailing and efficiency limitation in kesterite solar cells, Appl. Phys. Lett. 103 (2013) 103506, , https://doi.org/10.1063/1.4820250.

[9] K.G. Lisunov, M. Guk, A. Nateprov, S. Levcenko, V. Tezlevan, E. Arushanov, Features of the acceptor band and properties of localized carriers from studies of the variable-range hopping conduction in single crystals of p-Cu_2ZnSnS_4, Sol. Energy Mater. Sol. Cell 112 (2013) 127–133, https://doi.org/10.1016/j.solmat.2013.01.027.

[10] E. Lahderanta, M. Guc, M.A. Shakhov, E. Arushanov, K.G. Lisunov, Influence of scattering and interference effects on the low-temperature magnetotransport of Cu_2ZnSnS_4 single crystals, J. Appl. Phys. 120 (2016) 035704, https://doi.org/10.1063/1.4959107.

[11] E. Lähderanta, K. Lisunov, M.A. Shakhov, M. Guc, E. Hajdeu-Chicarosh, S. Levcenko, I. Zakharchuk, E. Arushanov, High-field hopping magnetotransport in kesterites, J. Magn. Magn. Mater. 459 (2018) 246–251, https://doi.org/10.1016/j.jmmm.2017.10.094.

[12] A. Walsh, S. Chen, S.-H. Wei, X.-G. Gong, Kesterite thin-film solar cells: advances in materials modelling of Cu_2ZnSnS_4, Adv. Energy Mater. 2 (2012) 400–409, https://doi.org/10.1002/aenm.201100630.

[13] S. Chen, A. Walsh, X.-G. Gong, S.-H. Wei, Classification of lattice defects in the kesterite Cu_2ZnSnS_4 and $Cu_2ZnSnSe_4$ earth-abundant solar cell absorbers, Adv. Mater. 25 (2013) 1522–1539, https://doi.org/10.1002/adma.201203146.

[14] H. Cui, X. Liu, F. Liu, X. Hao, N. Song, C. Yan, Boosting Cu_2ZnSnS_4 solar cells efficiency by a thin Ag intermediate layer between absorber and back contact, Appl. Phys. Lett. 104 (2014) 041115, , https://doi.org/10.1063/1.4863951.

[15] M. Pilvet, M. Kauk-Kuusik, M. Altosaar, M. Grossberg, M. Danilson, K. Timmo, A. Mere, V. Mikli, Compositionally tunable structure and optical properties of $Cu_{1.85}(Cd_xZn_{1-x})_{1.1}SnS_{4.1}$ ($0 \le x \le 1$) monograin powders, Thin Solid Films 582 (2015) 180–183, https://doi.org/10.1016/j.tsf.2014.10.091.

[16] V.P. Kumar, E. Guilmeau, B. Raveau, V. Caignaert, U.V. Varadaraju, A new wide band gap thermoelectric quaternary selenide $Cu_2MgSnSe_4$, J. Appl. Phys. 118 (2015) 155101, , https://doi.org/10.1063/1.4933277.

[17] S. Chen, J.H. Yang, X. Gong, A. Walsh, S.H. Wei, Intrinsic point defects and complexes in the quaternary kesterite semiconductor Cu_2ZnSnS_4, Phys. Rev. B 81 (2010) 245204, , https://doi.org/10.1103/PhysRevB.81.245204.

[18] Z.-K. Yuan, S. Chen, H. Xiang, X.-G. Gong, A. Walsh, J.-S. Park, I. Repins, S.-H. Wei, Engineering solar cell absorbers by exploring the band alignment and defect disparity: the case of Cu- and Ag-based kesterite compounds, Adv. Funct. Mater. 25 (2015) 6733–6743, https://doi.org/10.1002/adfm.201502272.

[19] E. Chagarov, K. Sardashti, A.C. Kummel, Y.S. Lee, R. Haight, T.S. Gershon, $Ag_2ZnSn(S,Se)_4$: a highly promising absorber for thin film photovoltaics, J. Chem. Phys. 144 (2016) 104704, , https://doi.org/10.1063/1.4943270.

[20] T. Gershon, Y.S. Lee, P. Antunez, R. Mankad, S. Singh, D. Bishop, O. Gunawan, M. Hopstaken, R. Haightet, Photovoltaic materials and devices based on the alloyed kesterite absorber $(Ag_xCu_{1-x})_2ZnSnSe_4$, Adv. Energy Mater. 6 (2016) 1502468, https://doi.org/10.1002/aenm.201502468.

[21] C.J. Hages, M.J. Koeper, R. Agrawal, Optoelectronic and material properties of nanocrystal-based CZTSe absorbers with Ag-alloying, Sol. Energy Mater. Sol. Cell 145 (2016) 342–348, https://doi.org/10.1016/j.solmat.2015.10.039.

[22] Y.-F. Qi, D.-X. Kou, W.-H. Zhou, Z.-J. Zhou, Q.-W. Tian, Y.-N. Meng, X.-S. Liu, Z.-L. Dua, S.-X. Wu, Engineering of interface band bending and defects elimination via a Ag-graded active layer for efficient $(Cu,Ag)_2ZnSn(S,Se)_4$ solar cells, Energy Environ. Sci. 10 (2017) 2401–2410, https://doi.org/10.1039/C7EE01405H.

[23] T. Gershon, K. Sardashti, O. Gunawan, R. Mankad, S. Singh, Y.S. Lee, J.A. Ott, A. Kummel, R. Haight, Photovoltaic device with over 5% efficiency based on an n-type $Ag_2ZnSnSe_4$ absorber, Adv. Energy Mater. 6 (2016) 1601182, , https://doi.org/10.1002/aenm.201601182.

[24] T.H. Nguyen, T. Kawaguchi, J. Chantana, T. Minemoto, T. Harada, S. Nakanishi, S. Ikeda, Structural and solar cell properties of a Ag-containing Cu_2ZnSnS_4 thin film derived from spray pyrolysis, ACS Appl. Mater. Inter. 10 (2018) 5455–5463, https://doi.org/10.1021/acsami.7b14929.

[25] M.H. Sayed, J. Schoneberg, J. Parisi, L. Gutay, Influence of silver incorporation on CZTSSe solar cells grown by spray pyrolysis, Mat. Sci. Semicond. Process. 76 (2018) 31–36, https://doi.org/10.1016/j.mssp.2017.12.007.

[26] W.-C. Huang, S.-Y. Wei, C.-H. Cai, C. Yeh, W.-H. Ho, C.-H. Lai, The role of Ag in aqueous solution processed $(Ag,Cu)_2ZnSn(S,Se)_4$ kesterite solar cells: antisite defect elimination and importance of Na passivation, J. Mat. Chem. A 6 (2018) 15170–15181, https://doi.org/10.1039/c8ta02950d.

[27] L. Dermenji, N. Curmei, M. Guc, G. Gurieva, M. Rusu, V. Fedorov, L. Bruc, D. Sherban, S. Schorr, A. Simashkevich, E. Arushanov, Effects of annealing on elemental composition and quality of CZTSSe thin films obtained by spray pyrolysis, Surf. Engineer. Appl. Electrochem. 52 (2016) 509–514, https://doi.org/10.3103/S1068375516060041.

[28] V. Duzhko, V.Yu. Timoshenko, F. Koch, Th. Dittrich, Photovoltage in nanocrystalline porous TiO_2, Phys. Rev. B 64 (2001) 075204, https://doi.org/10.1103/PhysRevB.64.075204.

[29] M. Guc, S. Levcenko, I.V. Bodnar, V. Izquierdo-Roca, X. Fontane, L.V. Volkova, E. Arushanov, A. Pérez-Rodríguez, Polarized Raman scattering study of kesterite type Cu_2ZnSnS_4 single crystals, Sci. Rep. 6 (2016) 19414, https://doi.org/10.1038/srep19414.

[30] M. Dimitrievska, A. Fairbrother, X. Fontane, T. Jawhari, V. Izquierdo-Roca, E. Saucedo, A. Perez-Rodriguez, Multiwavelength excitation Raman scattering

study of polycrystalline kesterite Cu_2ZnSnS_4 thin films, Appl. Phys. Lett. 104 (2014) 021901, , https://doi.org/10.1063/1.4861593.
[31] M. Dimitrievska, G. Gurieva, H. Xie, A. Carrete, A. Cabot, E. Saucedo, A. Pérez-Rodríguez, S. Schorr, V. Izquierdo-Roca, Raman scattering quantitative analysis of the anion chemical composition in kesterite $Cu_2ZnSn(S_xSe_{1-x})_4$ solid solutions, J. Alloy Compd. 628 (2015) 464–470, https://doi.org/10.1016/j.jallcom.2014.12.175.
[32] N.B.M. Amiri, A. Postnikov, Electronic structure and lattice dynamics in kesterite-type $Cu_2ZnSnSe_4$ from first-principles calculations, Phys. Rev. B 82 (2010) 205204, , https://doi.org/10.1103/PhysRevB.82.205204.
[33] E. Garcia-Llamas, M. Guc, I.V. Bodnar, X. Fontané, R. Caballero, J.M. Merino, M. León, V. Izquierdo-Roca, Multiwavelength excitation Raman scattering of $Cu_2ZnSn_{1-x}Ge_x(S,Se)_4$ single crystals for earth abundant photovoltaic applications, J. Alloy Compd. 692 (2017) 249–256, https://doi.org/10.1016/j.jallcom.2016.09.035.
[34] K.-W. Cheng, W.-T. Tsai, Y.-H. Wu, Photo-enhanced salt-water splitting using orthorhombic Ag_8SnS_6 photoelectrodes in photoelectrochemical cells, J. Power Sources 317 (2016) 81–92, https://doi.org/10.1016/j.jpowsour.2016.03.086.
[35] S. Levcenko, J. Just, A. Redinger, G. Larramona, S. Bourdais, G. Dennler, A. Jacob, T. Unold, Deep defects in $Cu_2ZnSn(S,Se)_4$ solar cells with varying Se content, Phys. Rev. Appl. 5 (2016) 024004, , https://doi.org/10.1103/PhysRevApplied.5.024004.
[36] M. Neuschitzer, M. Espindola Rodriguez, M. Guc, J. Marquez, S. Giraldo, I. Forbes, A. Perez-Rodriguez, E. Saucedo, Revealing the beneficial effects of Ge doping on $Cu_2ZnSnSe_4$ thin film solar cells, J. Mater. Chem. A 6 (2018) 11759–11772, https://doi.org/10.1039/C8TA02551G.
[37] M. Guc, M. Espíndola Rodríguez, L.I. Bruc, K.G. Lisunov, L. Dermenji, N. Curmei, D.A. Sherban, A.V. Simashkevich, E. Saucedo, A. Perez-Rodriguez, E.K. Arushanov, Transport properties of kesterite thin films of Cu_2ZnSnS_4 obtained by spray pyrolysis, 28th European Photovoltaic Solar Energy Conference and Exhibition, 2013, pp. 2449–2452, , https://doi.org/10.4229/28thEUPVSEC2013-3BV.6.55.
[38] M. Guc, R. Caballero, K.G. Lisunov, N. López, E. Arushanov, J.M. Merino, M. León, Disorder and variable-range hopping conductivity in Cu_2ZnSnS_4 thin films prepared by flash evaporation and post-thermal treatment, J. Alloys Compd. 596 (2014) 140–144, https://doi.org/10.1016/j.jallcom.2014.01.177.